DEVELOPMENT OF THE EMPIRICAL MODEL FOR RICE FIELD DISTRIBUTION MAPPING USING MULTI-TEMPORAL LANDSAT ETM+ DATA: CASE STUDY IN BALI INDONESIA

I.W. Nuarsa [a,b,*], F. Nishio [a] and C. Hongo [a]

[a] Center for Environmental Remote Sensing, Chiba University, Chiba 263-8522, Japan – fnishio@faculty.chiba-u.jp (F. Nishio.); hongo@faculty.chiba-u.jp (C. Hongo)

[b] Agroecotechnology Department, Faculty of Agriculture, Udayana University, Bali, Indonesia – nuarsa@ymail.com

Commission VIII, WG VIII/6

KEY WORDS: Rice field, Mapping, Empirical model, Multi-temporal, Landsat

ABSTRACT:

Information about an area and its distribution of planted and harvested paddy rice field is essential for food security management, water resource management, and for the estimation of gas emissions. Rice field has specific coverage characteristics throughout its life time. Its coverage is mixed proportionally in accordance with its age, between water, soil, and rice vegetation. Landsat ETM+ has a good spatial, spectral, and temporal resolution for rice growth monitoring and production estimation. The study was done in Tabanan Regency, Bali Province, Indonesia. The objectives of the study were: (1) to develop the rice growth vegetation index (RGVI), (2) to map the rice distribution and its age, and (3) to quantitative compare the rice field area's analysis results with the reference data. The results of this study show that an exponential equation is the best relationship form between a rice field spectral and the rice age. The visible bands of Landsat ETM+ (Band 1, Band 2, and Band 3) show a weak exponential relationship with the rice age. However, the reflective infrared bands of Landsat ETM+ (Band 4 and B5) and the entire vegetation index show a strong exponential relationship with the rice age. Using multiple bands of Landsat ETM+ as a vegetation index gives a better result than using a single band. RGVI is the new vegetation index developed in this study with the equation RGVI = 1 – ((b1+b3)/(b4+b5+b7)) where b1, b3, b4, and b5 are the bands of Landsat ETM+. The RGVI that is evaluated in this study is the better vegetation index compared to the existing vegetation index. The relationship between rice age and RGVI shows the highest determination coefficient (R2) with the equation $y = 14.265e^{2.452x}$, where y and x are the rice age and RGVI respectively. Quantitative comparison of the rice field analysis results and reference data at district level shows a linear relationship with the equation y = 0.920x - 3.841 and R^2 = 0.971, where y is rice field area of reference data and x is the rice field area of the analysis result of the Landsat ETM+. The standard of this estimation is 43.04 ha.*

1. INTRODUCTION

Rice is one of the world's major staple foods and paddy rice field account for approximately 15% of the world's arable land (IRRI, 1993). In Indonesia, rice is one of the most important agriculture plants because rice is the main food of Indonesian people. Food security has long been an important political goal in Indonesia. This goal is most commonly associated with rice self-sufficiency. In the mid-1980s Indonesia briefly achieved 100% self-sufficiency for rice. However, growth of rice production slowed in the 1990s, leading to an increase in imports and a lower self-sufficiency ratio. Over the past two years the rice self-sufficiency ratio has remained around 95%, but dropped below 90% during the El Niño drought of 1998 (Bappenas, 2002).

Satellite remote sensing has been widely applied and has been recognized as a powerful and effective tool in detecting land use and land cover change (Ehlers et al., 1990; Meaille and Wald, 1990; Westmoreland and Stow, 1992; Harris and Ventura, 1995). Satellite remote sensing provides cost-effective multi-spectral and multi-temporal data (Paine, 1981). Satellite imagery has been used to monitor discrete land cover types by spectral classification. Additionally, it has been utilized to estimate biophysical characteristics of land surfaces via linear relationships with spectral reflectance or vegetation indices (Steininger, 1996; Nuarsa et al, 2005).

The study of using of satellite imagery to monitor the rice growth has been done (Shao et al, 1997; Kuroso et al, 1997; Le Toan at all, 1997; Panigrahy and Sharma, 1997; Oette et al, 2000; Shao et al, 2001; David et al, 2003). Some of the previous researches have used global and moderate image resolution such as NOAA AVHRR and MODIS to monitor rice field (Fang et al, 1998; Wataru et al, 2006; Xiao et al, 2005). However, the use of moderate and global spatial resolution satellite images has been restricted particularly in the small rice areas, because there are many kinds of land cover in one pixel. This will reduce the accuracy of assessment (Strahler et al, 2006). On the other hand, utilization of the fine or medium spatial resolution satellite images has been limited, especially in a session plant, due to fewer images being available over the entire 120 days growth period of the rice (Currey et. al., 1987). Landsat ETM+ has a good temporal, spatial, and spectral resolution for rice monitoring. The revisit time of Landsat ETM+ is 16 days with a spatial resolution of 30 m. Landsat ETM+ has six bands with

* Corresponding author. Email address: nuarsa@ymail.com

the same pixel size. This becomes beneficial in the development of the algorithm for rice modelling.

The objectives of the study are: (1) to develop the rice growth vegetation index (RGVI), (2) mapping of the rice distribution and its age, and (3) a quantitative comparison of the analysis result with the reference data of a rice field area.

2. STUDY AREA, DATA, AND METHOD

2.1 Description of the study area

The study was done in the Tabanan Regency, Province of Bali, Indonesia, centered at latitude 8°29'46" S longitude 115°29'48" E (Figure 1). The Tabanan Regency was selected for the study area due to Tabanan being the central production area of rice in Bali. Irrigated paddy rice area in Bali is not only used for rice cultivation, but also for other seasonal agriculture crops such as corn, soybean, etc. Plantation of rice in Bali is coordinated by the social farmer organization namely *Subak*. It is responsible for the managing of agriculture water resources. Each Subak area usually consists of around 150 - 300 ha of paddy rice area. In each *Subak*, farmers plant rice at the same time. Therefore, identification of agricultural rice area from space using remote sensing data such as Landsat ETM+ is made easier. This study used three Subaks in three different districts, Bengkel Subak in Kediri district, Sungi Subak in Marga District, and Risaja Subak in Penebel District. Field observations were done at 9 station points. The elevation of the stuy area range from 30 – 290 m asl. All of rice field observed used the Ciherang rice variety with a life cycle of around 115 days and the yield reaching 5.0 tons/ha.

Figure. 1. Location map of the study area.

Landsat Image Data

The Landsat satellite image has 8 bands including the thermal and panchromatic bands. In the visible, near infrared and middle infrared, Landsat ETM+ has a 30 m spatial resolution. However in the thermal and panchromatic region, the spatial resolutions are 60 m and 15 m respectively. In this study the visible and reflectance infrared (Band 1 - Band 5 and Band7) of Landsat ETM+ are used. Although the Landsat ETM+ used in this study has the SLC-off, considerations of the better spatial, spectral, and temporal resolution of this image still makes it relatively useful. With the 16 days of temporal resolution, Landsat ETM+ is the ideal satellite image for rice monitoring due to rice having an only 115 days of a growth cycle. The total of the Landsat images used in this study in two different years, 2002 and 2005, is 8 scenes. Landsat images of 2005 were used for rice modeling and those of 2002 were utilized to apply the rice field distribution mapping model

2.2 Data Analysis

Radiometric Corrections

In temporal analysis of the remote sensing data, radiometric corrections are an important part of the image analysis. The Digital number (DN) of the Landsat ETM+ at different acquisition dates should be converted to the corrected digital number (cDN) to eliminate the radiometric and atmospheric effects, so that they have comparable values. In this study, we used the simple radiometric correction model introduced by Pons and Solé-Sugrañes (1994). The formula of this model is shown in the following equation:

$$cDN = 1000a(DN - K_l)d^2/[\mu_s S_0 e^{(-\tau_0/\mu_0)} e^{(-\tau_0/\mu_v)}] \quad (1)$$

(i) (if $250 < cDN \leq 318.3$; $cDN = 254$),
(ii) (if $cDN > 318.3$; $cDN = 255$),
(iii) (if $\mu_s \leq 0$; $cDN = 255$),

where cDN = corrected digital number
a = gain value of each Landsat band
DN = digital number
K_l = radiances value of zone totally in shade
d = actual Sun-Earth distance
μ_s = cosine of the incident angle
S_0 = exoatmospheric solar irradiance
τ_0 = optical depth of the atmosphere
μ_0 = cosine of the solar zenith angle
μ_v = cosine of sensor view angle

cDN is the conversion of the effective reflectance to the common 8-bit format of most image processors. The range of the output values has been limited to between 0 and 255. Note that a, K_l, S_0, and τ_0 depend on the wavelength and have a different value for each spectral band; K_l depends varies for each image because it is related to and depends on atmospheric conditions; μ_0 and μ_s, depend on latitude, date, and time of the satellite pass; besides that, μ_s also depends on slope and aspect of each pixel; d depends on the date of the satellite pass, and μ_v depends on the sensor viewing angle. The parameter μ_v is 1 in most Landsat images because v is 0 at the nadir and has small values on the rest of the image (Pons and Solé-Sugrañes, 1994).

Practically, to apply the algorithm above we only need a DEM of enough quality (altimetrically and planimetrically) because all of the other parameters are known (e.g., S_0) or can be inferred from images (e.g.,K_l). To avoid overcorrections and undercorrections on the ridges and channels and to account for local phenomena, it is important to use a DEM with a planimetric resolution comparable to the geometric resolution of the image. Naugle and Lashlee (1992) showed that a DEM of 95 m can be insufficient for a Landsat TM image over rugged

terrain. In this study, we derived a DEM from the topographical map with a spatial resolution of 30 m.

Determining the relationship between rice spectral and rice age

Gathering cDN values from the Landsat pixels for the ninth observation site over the whole of rice growth time was the next step of data analysis. In each image and at each acquisition date, a 100 pixels sample randomly was taken in the ninth field observation site. The average value of the sample was used as a representative of the cDN value at that acquisition date. Relationship calculations between rice age and rice plant spectral are done for both band spectral of Landsat ETM+ and vegetation index with the following equation:

$$y = f(x) \quad (2)$$

where y is the rice age and x is the rice spectral. Several vegetation indexes evaluated in the study are Normalized Difference Vegetation Index (NDVI), Ratio Vegetation Index (RVI), Infrared Percentage Vegetation Index (IPVI), Difference Vegetation Index (DVI), Transformed Vegetation Index (TVI), and Soil Adjusted Vegetation Index (SAVI).

The relationship between rice age and both cDN and vegetation index was evaluated using the statistical parameters. These are: the determination coefficient (R^2), the significant value of of variance analysis (ANOVA), and the standard error of estimation (SE). The highest R^2, lowest significant value of ANOVA, and lowest standard error of estimation of relationship between rice age and Landsat spectral of rice were selected and used for rice field mapping model.

Development of Rice Growth Vegetation Index (RGVI)

Theoretically, rice plant in normal condition is the same as vegetation in general. Chlorophyll pigments that are present in leaves absorb red light. In the NIR portion, radiation is scattered by the internal spongy mesophyll leaf structure, which leads to higher values in the NIR channels. This interaction between leaves and the light that strikes them is often determined by their different responses in the red and NIR portions of reflective light (Niel and McVicar, 2001). On the other hand, absorption properties of the middle infrared band cause low reflectance of rice plant in this channel (Lilliesand and Kiefer, 1994). In irrigated rice field, especially in early transplanting period, the water environment of rice plays an important role in the rice spectral. The Blue band of Landsat ETM+ has a good sensitivity to the existence of water. Therefore, in the development of the rice growth vegetation index (RGVI) in this study B1, B3, B4, and B5 of Landsat ETM+ were used in the following equation.

$$RGVI = 1 - \frac{(B1 + B3)}{(B4 + B5 + B7)} \quad (3)$$

where RGVI = the rice growth vegetation index
B1, B3, B4, B5, and B7 = band of Landsat ETM+.

Mapping rice field and its age

At least two Landsat image with sequential acquisition dates were used in the following procedures to map the distribution of rice field.

1. Converting the cDN of Landsat image to rice age using the best relationship equation between rice age and Landsat spectral for both Landsat image in sequential acquisition date. This procedure will produce two rice field maps age_t and Age_{t+n}.
2. Calculating the age difference (Δage) of two Landsat images with the equation bellow.

$$\Delta age = age_{t+n} - age_t \quad (4)$$

where Δage = maps of difference rice age of two sequential acquisition dates of Landsat image
Age = rice age map in t acquisition date
Age_{t+n} = rice age map in t + n day of acquisition date.

3. Calculating the time period (days) of sequential acquisition dates (Δt).
4. Comparing Δage and Δt. The pixels that satisfy the following equation within the standard error of calculation (SE) are classified as rice field with the equation below.

$$\Delta age - SE \leq \Delta t \leq \Delta age + SE \quad (5)$$

3. RESULTS AND DISCUSSION

3.1 The Relationship between rice spectral and rice age

The average cDN value of the rice field at several ages over its entire life is shown in Table 1, while the average value of its vegetation index is displayed in Table 2. In general, the rice field spectral increases from the beginning of the transplanting period until rice age of two months and it decreases until the end of its age. This trend is similar for both cDN and vegetation index, except Band 3 and TVI that show a reverse tendency.

Age	cDN1	cDN2	cDN3	cDN4	cDN5	cDN7
5	76.14	47.45	44.01	47.33	27.63	15.94
12	74.32	48.74	42.95	51.65	32.95	17.73
17	88.91	55.19	50.35	70.30	44.64	24.88
31	65.20	46.16	36.61	99.76	59.53	28.46
42	63.38	42.28	32.39	122.99	65.91	29.35
50	72.50	42.93	31.33	138.12	74.42	30.25
54	68.85	43.57	30.28	151.09	77.48	31.14
70	67.03	46.80	32.39	140.28	68.04	27.57
73	63.38	47.45	34.50	133.80	69.10	26.67
77	70.67	50.03	42.95	125.15	71.23	25.78

Table 1. Average cDN of the rice field for several rice ages

Age	NDVI	RVI	IPVI	DVI	TVI	SAVI	RGVI
5	0.04	1.08	0.52	3.32	136.54	0.05	-0.32
12	0.09	1.20	0.55	8.70	129.97	0.14	-0.15
17	0.09	1.20	0.55	9.95	130.19	0.13	-0.07
31	0.37	2.18	0.69	43.14	107.17	0.55	0.39
42	0.58	3.80	0.79	90.60	96.09	0.87	0.56
50	0.63	4.41	0.82	106.79	94.06	0.94	0.57
54	0.67	4.99	0.83	120.82	92.60	1.00	0.62
70	0.63	4.33	0.81	107.90	94.29	0.94	0.58
73	0.59	3.88	0.80	99.30	95.78	0.88	0.57
77	0.49	2.91	0.74	82.20	100.56	0.73	0.49

Table 2. Average vegetation index of the rice field for several rice ages

Based on statistical analysis, exponential is the best equation form to show the relationship between rice field spectral and rice age. The best exponential relationship between rice age and rice cDN was given by Band 5 (Figure 2) followed by Band 4, and Band 7 of Landsat ETM+ with the determination coefficients (R^2) being 0.8999, 0.8721, and 0.6847 respectively. Band 1, Band 2, and Band 3 show a weak relationship with the rice age with the R^2 being 0.3325, 0.0973, and 0.3994 respectively. On the other hand, using multiple bands of Landsat ETM+ as a vegetation index gave a better relationship between rice age and rice spectral than utilized a single band. All vegetation indexes evaluated in this study showed strong relationships with rice age. The Rice Growth Vegetation Index (RGVI) developed in this study gives the best relationship with the R^2 being 0.9043 (Figure 3), followed by TVI, NDVI, SAVI, IPVI, DVI, and RVI with the R^2 being 0.8888, 0.8473, 0.847, 0.8465, 0.8307, and 0.7112 respectively.

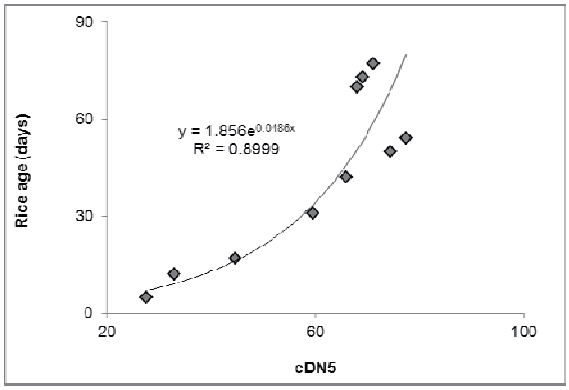

Figure 2. Relationship between rice cDN of Landsat ETM+ and rice age of Band 5.

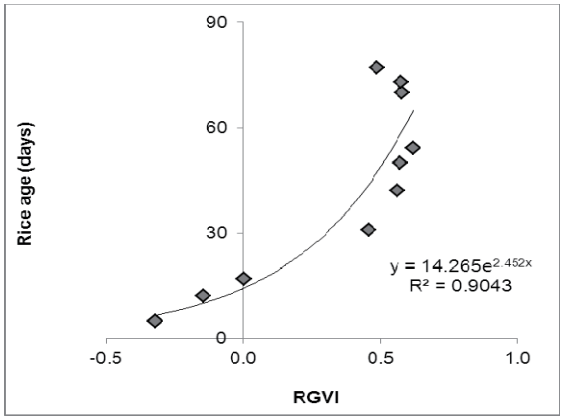

Figure 3. Relationship between rice vegetation index and rice age of RGVI.

The advantages of using the vegetation index compared to using a single band is the reduction of the spectral data to a single number that is related to the physical characteristics of vegetation (e.g. leaf area, biomass, productivity, photosynthetic activity, or percent cover) (Baret and Guyot, 1991; Huete, 1988), while minimizing the effect of internal (e.g. canopy geometry, and leaf and soil properties) and external factors (e.g. sun-target-sensor angles, and atmospheric conditions at the time of image acquisition) on the spectral data (Baret and Guyot, 1991; Huete and Warrick, 1990; Huete and Escadafal, 1991).

3.2 Rice field mapping

According to the statistical analysis of the relationship between rice spectral and rice age, RGVI is the best vegetation index to track the rice age due to it having the highest value of R^2 and the lowest significant value of analysis of variance (Sig) and standard error of estimation (SE) (Table 3). Therefore, the exponential equation formula of RGVI to be used for rice field mapping is:

$$y = 14.265e^{2.452x} \quad (6)$$

where y = the rice age
e = the natural logarithm
x = RGVI

Rice Spectral	R^2	Sig	SE
cD1	0.3325	0.081	0.787
cD2	0.0973	0.380	0.915
cD3	0.3994	0.050	0.746
cD4	0.8254	0.000	0.402
cD5	0.8999	0.000	0.305
cD7	0.6847	0.003	0.541
NDVI	0.8259	0.000	0.402
RVI	0.6855	0.003	0.540
IPVI	0.8250	0.000	0.403
DVI	0.7929	0.001	0.438
TVI	0.8702	0.000	0.347
SAVI	0.8254	0.000	0.402
RGVI	0.9045	0.000	0.297

Table 3. Values of determination coefficient, significant, and standard error in calculations of the relationship between rice spectral and rice age.

Rice field age was estimated using equation 5 for two sequential acquisitions date of Landsat ETM+. The pixels that have the same difference value between predicted rice age in two sequential acquisitions date and the day distinction of two sequential acquisitions dates is classified as a rice field area after the standard error of estimation is included.

Figure 4 and Table 4 show the distribution of the rice area resulting from the classification process using equation 5. The map of figure 4 is not only describing the distribution of rice field but also its age. This information is important to estimate the total amount of rice field that can be harvested.

District	nPixel	Area (ha)
Kerambitan	6701	603.09
Selemadeg	7812	703.08
Pupuan	884	79.56
Tabanan	2152	193.68
Kediri	5762	518.58
Marga	3091	278.19
Penebel	1585	142.65
Baturiti	2149	193.41

Table 4. Rice field area of analysis results of each district

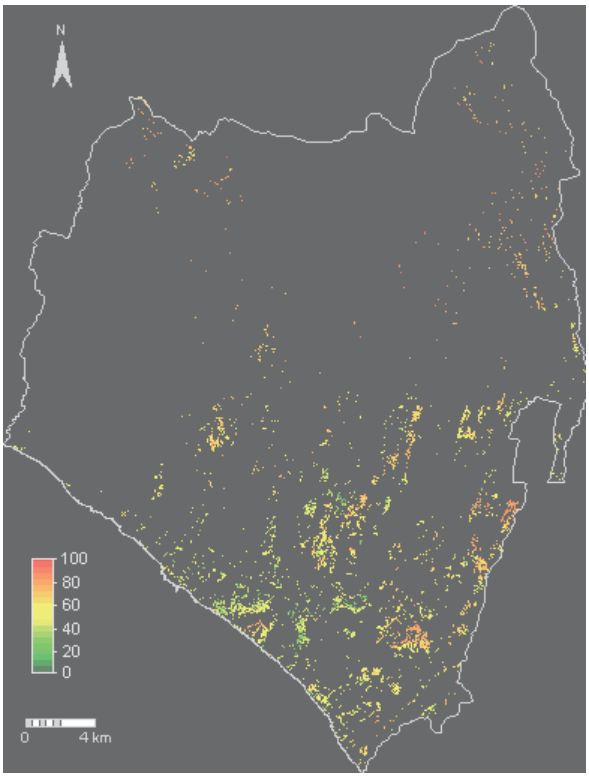

Figure 4. Rice field distribution map of the study area resulting from the analysis of Landsat ETM+ data

3.3 Quantitative evaluation of the Landsat-derived rice field map

Quantitative evaluation of Landsat ETM+ accuracy for rice mapping and harvest time distribution have been done by comparing the total area derived from Landsat ETM+ and the data released by the Statistic Center Agency. The Agriculture Department of Local Government did not publish the spatial data for land that was being planted with the rice. Therefore, the evaluations of the study result have been carried out using a district-level comparison. Table 5 shows comparisons of total rice area analysis results of Landsat ETM+and reference data.

District	Analysis Result (ha)	Reference data (ha)	Difference (%)
Kerambitan	603.09	560	-7.69%
Selemadeg	703.08	809	13.09%
Pupuan	79.56	95	16.25%
Tabanan	193.68	203	4.59%
Kediri	518.58	591	12.25%
Marga	278.19	314	11.40%
Penebel	142.65	165	13.55%
Baturiti	193.41	242	20.08%

Table 5. Comparison in district level of rice area between analysis results of Landsat ETM+ and reference data

Based on Table 5, total rice area that was planted was under-estimated for all districts, except for the Kerambitan district. For the Districts of Selemadeg, Pupuan, Tabanan, Kediri, Marga, Penebel, and Baturoti, the total of area estimated from the Landsat data is lower by amounts of 13.09%, 16.25%, 4.59%, and 12.25%, 11.40%, 13.55% and 5.69% respectively compared to the Statistic Center Agency data. However, in Kerambitan District the estimation result from Landsat images is greater than the reference data by around 7.69%. The under-estimation for almost all rice areas obtained from Landsat images compared to the data from the local government is caused by some of the Landsat rice pixels containing several objects other than rice field. The mixed pixels can decrease the accuracy of the calculation (Strahler *et al*, 2006). Xiao *et al* (2005) has come across the same phenomena using the MODIS data. They carried out that the estimation of the rice field area in the Southern China using MODIS images, with results lower than the references data.

The estimated rice area of Landsat ETM+ and the reference data show a strong relationship. The determination coefficient (R^2) was 0.971 with the equation y = 0.920x - 3.841, where y is estimation area from the Landsat ETM+ and x is the reference data area (Figure 5). The standard error of the estimation is 43.04 ha.

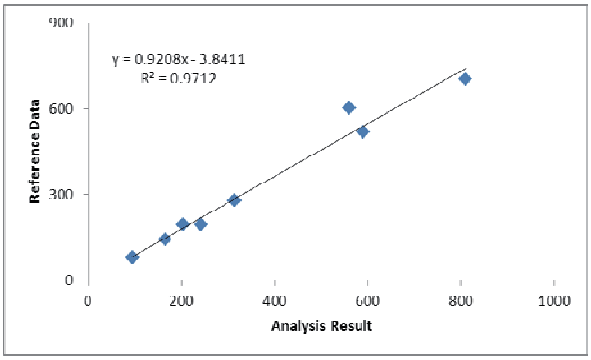

Figure 5. District-level comparison of the rice area from the Landsat ETM+ and the data from the Local Government.

4. CONCLUSIONS

1. The Visible bands of Landsat ETM+ (Band1, Band 2, and Band 3) show a weak exponential relationship with the rice age. However, the reflective infrared bands of Landsat ETM+ (Band 4, Band 5, and B 7) and the entire vegetation index show a strong exponential relationship with the rice age. Using the vegetation indexes to monitor and map rice field gives better results that only use a single band of Landsat ETM+.
2. The Rice Growth Vegetation Index (RGVI) is the new vegetation index developed in this study. RGVI is a better vegetation index to describe rice age than exiting vegetation indexes evaluated in this study. The relationship between rice age and RGVI has shown the highest determination coefficient (R^2) with the equation $y = 14.265e^{2.452x}$, where y and x is the rice age and RGVI respectively.
3. Quantitative comparison of the rice field analysis result and reference data at district level show a linear

relationship with the equation y = 0.920x - 3.841 and R^2 = 0.971, where y is rice field area of reference data and x is the rice field area of the analysis result of the Landsat ETM+. The standard error of this estimation is 43.04 ha.

4. Landsat ETM+ has good capabilities of monitoring and mapping of the rice field.

References

Bappenas, 2002, Does Indonesia Face a Food Security Time Bomb? *Indonesian Food Policy Program*. http//:www.macrofoodpolicy.com. Accessed November, 15th 2009.

Baret, F. and Guyot, G., 1991, Potentials and limits of vegetation indices for LAI and APAR assessment. *Remote Sensing of Environment*, 35, pp. 161-173.

Currey, B., Fraser, A. S. and Bardsley, K. L. How useful is Landsat monitoring. Nature 1987, 328, 587-590.

David, D., Frolking, S., Li, C., 2003, Trends in Rice-Wheat Area in China. *Field Crops Research*.

Ehlers, M., Jadkowski, M. A., Howard, R. R. and Brostuen, D. E., 1990, Application of SPOT data for regional growth analysis and local planning. *Photogrammetric Engineering and Remote Sensing*, 56, pp. 175–180.

Fang, H., Wu, B., Liu, H., and Huang, X., 1998, Using NOAA AVHRR and Landsat TM to estimate rice area year-by-year. *International Journal of Remote Sensing*, 19, pp. 521-525.

Harris, P. M. and Ventura, S. J., 1995, The integration of geographic data with remotely sensed imagery to improve classification in an urban area. *Photogrammetric Engineering and Remote Sensing*, 61, pp. 993–998.

Huete, A. R., 1988, A soil-adjusted vegetation index (SAVI). *Remote Sensing of Environment* , 25, pp. 295-309.

Huete, A. R. and Escadafal, R., 1991, Assessment of biophysical soil properties through spectral decomposition techniques. *Remote Sensing of Environment* 35, pp. 149-159.

Huete, A. R. and Warrick, A. W., 1990, Assessment of vegetation and soil water regimes in partial canopies with optical remotely sensed data. *Remote Sensing of Environment* 32, pp. 115-167.

IRRI, 1993, *1993–1995 IRRI Rice Almanac*. Manila7 International Rice Research Institute.

Kuroso, T., Fujita, M., and Chiba, K., 1997, Monitoring of Rice Fields Using Multi-Temporal ERS-1 C-band SAR Data. *International Journal of Remote Sensing*, 14, pp. 2953-2965.

Le Toan, T., Ribbes, F., Floury, N., L., Kong, J., Korosu, T., and Fujita, M., 1997, Rice Crop Mapping and Monitoring Using ERS-1 Data Base on Experiment and Modeling Results. *IEEE Transactions on Geosciences and Remote Sensing*, 35, pp. 41- 56.

Lillesand, T.M. and Kiefer, R.W., 1994, *Remote Sensing and Image Interpretation*. Third Edition. John Wiley and Sons, New York. 750 pp.

Meaille, R. and Wald, L., 1990, Using geographic information system and satellite imagery within a numerical simulation of regional urban growth. *International Journal of Geographic Information Systems*, 4, pp. 445–456.

Naugle, B. I. and Lashlee, J. D., 1992, Alleviating topographic influences on land-cover classifications for mobility and combat modeling, *Photogrammetric Engineering and Remote Sensing*, 58, pp. 1217-1221.

Niel, T.G.V. and McVicar, T.R., 2001, Remote Sensing of Rice-Based Irrigated Agriculture: A Review. Available on http://www.clw.csiro.au/publications/consultancy/2001/CRC-Rice-TRP11050101.pdf. Accessed 15 December 2009.

Nuarsa I Wayan, Kanno, S., Sugimori, Y. and Nishio, F., 2005, Spectral Characterization of Rice Field Using Multi-Temporal Landsat ETM+ Data. *International Journal of Remote Sensing and Earth Sciences*. 2, pp. 65-71.

Oette, D. R., Warren B. C., Mercedes B., Maiersperger, T.K., and Kennedy, R.E., 2000, Land Cover Mapping in Agricultural Setting Using Multiseasonal Thematic Mapper Data. *Remote Sensing of Environment*, 76, pp. 139-155.

Paine, D.P., 1981, *Aerial Photography and Image Interpretation for Resource Management*. John Wiley and Sons, New York. 412 pp.

Panigrahy, S. and Sharma., S.A., 1997, Mapping of Crop Rotation Using Multidate Indian Remote Sensing Satellite Digital Data. *ISPRS Journal of Photogrammetry & Remote Sensing*, 52, pp. 85-91.

Pons, X. and Solé-Sugrañes, L. A simple radiometric correction model to improve automatic mapping of vegetation from multispectral satellite data. Remote Sensing of Environment 1994, 48, 191-204.

Shao, Y., Fan, X., Liu, H., Xiao, J., Ross, S., Brisco, B., Brown, R. and Staples, G., 2001. Rice Monitoring and Production Estimation Using Multitemporal RADARSAT. *Journal of Remote Sensing for Environment*, 76, pp. 310–325.

Shao, Y., Wang, C., Fan, X., and Liu, H., 1997, Evaluation of SAR image for Rice Monitoring and Land Cover Mapping. In Presented at *Geomatics in Era of RADARSAT*, Ottawa, Canada.

Steininger, M. K., 1996, Tropical secondary forest regrowth in the Amazon: age, area and change estimation with Thematic Mapper data. *International Journal of Remote Sensing*, 17, pp. 9–27.

Strahler, A. H., Boschetti, L., Foody, G.M., Friedl, M.A., Hansen, M.C., Herold, M., Mayaux, P., Morisette, J.T., Stehman, S.V. and Woodcock, C.E., 2006, Global Land Cover Validation: Recommendations for Evaluation and Accuracy Assessment of Global Land Cover Maps. *Office for Official Publications of the European Communities*. http://wgcv.ceos.org/docs/plenary/wgcv26/GlobalLandCover Validation_JeffMorisette.pdf. Accessed July 25, 2009.

Wataru, T, Taikan, O., and Yoshifumi, Y., 2006, Investigating an integrated approach on rice paddy monitoring over Asia with MODIS and AMSR-E. *Proceedings of the Conference of the Remote Sensing Society of Japan*, 40, pp. 173-174.

Westmoreland, S. and Stow, D. A., 1992, Category identification of changed land-use polygons in an integrated image processing/geographic information system. *Photogrammetric Engineering and Remote Sensing*, 58, pp. 1593–1599.

Xiao, X., Boles, S., Liu, J., Zhuang, D., Frolking, S., Li, C., Salas, W. and Moore, B., 2005, Mapping paddy rice agriculture in southern China using multi-temporal MODIS images. *Remote Sensing of Environment*, 95, pp. 480–492.